Received: 28 November 2023 | Revised: 2 March 2024 | Accepted: 13 March 2024

DOI: 10.1002/hbm.26670

RESEARCH ARTICLE

WILEY

Altered intersubject functional variability of brain white-matter in major depressive disorder and its association with gene expression profiles

Qun Gai[1,2,3] | Tongpeng Chu[1,2,3] | Qinghe Li[4] | Yuting Guo[4] | Heng Ma[1] | Yinghong Shi[1] | Kaili Che[1] | Feng Zhao[5] | Fanghui Dong[4] | Yuna Li[6] | Haizhu Xie[1] | Ning Mao[1,2,3]

[1]Department of Radiology, Yantai Yuhuangding Hospital, Qingdao University, Yantai, Shandong, China

[2]Big Data & Artificial Intelligence Laboratory, Yantai Yuhuangding Hospital, Yantai, Shandong, China

[3]Shandong Provincial Key Medical and Health Laboratory of Intelligent Diagnosis and Treatment for Women's Diseases, Yantai Yuhuangding Hospital, Yantai, Shandong, China

[4]School of Medical Imaging, Binzhou Medical University, Yantai, Shandong, China

[5]School of Computer Science and Technology, Shandong Technology and Business University, Yantai, Shandong, China

[6]Department of Radiology, Beijing Tiantan Hospital, Capital Medical University, Beijing, China

Correspondence
Haizhu Xie and Ning Mao, Department of Radiology, Yantai Yuhuangding Hospital, Qingdao University, Yantai, Shandong, 264000, China.
Email: xhz000417@sina.com and maoning@pku.edu.cn

Funding information
Taishan Scholar Foundation of Shandong Province, Grant/Award Number: tsqn202211378; Natural Science Foundation of Shandong Province, Grant/Award Numbers: ZR2023QH084, ZR2023QH107; National Natural Science Foundation of China, Grant/Award Numbers: 62176140, 82371933

Abstract

Major depressive disorder (MDD) is a clinically heterogeneous disorder. Its mechanism is still unknown. Although the altered intersubject variability in functional connectivity (IVFC) within gray-matter has been reported in MDD, the alterations to IVFC within white-matter (WM-IVFC) remain unknown. Based on the resting-state functional MRI data of discovery (145 MDD patients and 119 healthy controls [HCs]) and validation cohorts (54 MDD patients, and 78 HCs), we compared the WM-IVFC between the two groups. We further assessed the meta-analytic cognitive functions related to the alterations. The discriminant WM-IVFC values were used to classify MDD patients and predict clinical symptoms in patients. In combination with the Allen Human Brain Atlas, transcriptome-neuroimaging association analyses were further conducted to investigate gene expression profiles associated with WM-IVFC alterations in MDD, followed by a set of gene functional characteristic analyses. We found extensive WM-IVFC alterations in MDD compared to HCs, which were associated with multiple behavioral domains, including sensorimotor processes and higher-order functions. The discriminant WM-IVFC could not only effectively distinguish MDD patients from HCs with an area under curve ranging from 0.889 to 0.901 across three classifiers, but significantly predict depression severity ($r = 0.575$, $p = 0.002$) and suicide risk ($r = 0.384$, $p = 0.040$) in patients. Furthermore, the

Qun Gai and Tongpeng Chu are co-first authors in this study.

variability-related genes were enriched for synapse, neuronal system, and ion channel, and predominantly expressed in excitatory and inhibitory neurons. Our results obtained good reproducibility in the validation cohort. These findings revealed intersubject functional variability changes of brain WM in MDD and its linkage with gene expression profiles, providing potential implications for understanding the high clinical heterogeneity of MDD.

KEYWORDS
functional connectivity, intersubject variability, major depressive disorder, transcriptomics, white-matter

1 | INTRODUCTION

Major depressive disorder (MDD) is a highly prevalent psychiatric disorder and a major cause of disability (DALYs & Collaborators, 2018). According to the World Health Organization, MDD will be the leading cause of disease burden worldwide by 2030 (Lepine & Briley, 2011). MDD is known to be a clinically heterogeneous disorder characterized by a mixture of emotional, cognitive, and autonomic symptoms (Malhi & Mann, 2018). Although growing studies reported structural and functional brain alterations in MDD (Zhuo et al., 2019), our current understanding of its pathophysiology is unclear with inconsistent findings across studies. This hampers the discovery of reliable neuroimaging-based biomarkers that can guide clinical diagnosis and optimize treatment. One major reason for this situation is that most prior MDD studies have utilized case–control designs to evaluate mean group differences between patients and healthy controls (HCs), ignoring the intersubject differences among patients with MDD.

As an advanced neuroimaging technique, resting-state functional MRI (rs-fMRI) provides an unprecedented opportunity to noninvasively investigate the brain functional connectivity (FC), which is based on the temporal synchronization of blood-oxygenation-level-depend (BOLD) signals between pairs of brain regions (Biswal et al., 1995). Recently, a great deal of evidence supports that this inter-regional FC architecture is unique among individuals and reflects individual differences in cognitive or behavior (Li, Wei, et al., 2021; Smith et al., 2015). Therefore, an increasing body of rs-fMRI studies have moved towards characterizing the intersubject variability in FC (IVFC) (Horien et al., 2019; Mueller et al., 2013). It has been reported that IVFC within gray-matter (GM-IVFC) exhibited a sizeable regional variability in HCs, with significantly higher variability in high-order cognitive networks and lower variability in lower-order perceptual networks (Li, Wei, et al., 2021). A meta-analysis further revealed that the regions with high IVFC have important value in identifying individuals and predicting higher cognitive functions (Finn & Todd Constable, 2016). In addition, GM-IVFC has been reported in some psychiatric and neurological disorders, including—but not limited to—schizophrenia (Sun et al., 2021), epilepsy (Dumlu et al., 2020) and MDD (Hou et al., 2023). For instance, Chen et al. reported greater heterogeneity in the visual cortex in both schizophrenia and MDD patients compared to HCs (Sun et al., 2021). Hou et al. found that the MDD group had increased IVFC in 33 GM regions of six brain networks (Hou et al., 2023). Overall, these findings highlight the implications of IVFC.

White-matter (WM), another fundamental component of the neural system, serves as the conduit for neural signal transmission between GM regions (Fields, 2008). However, its variabilities in connectome organization across individuals have been relatively unexplored. In recent years, emerging evidence has demonstrated a reliable detection of BOLD signals in WM. Ji et al. found that low-frequency BOLD fluctuations in WM exhibited a specific rather than a random distribution of noise (Ji et al., 2017). It has been reported that WM functional connectomes can predict individual general fluid intelligence to explore brain-behavior relationships (Li, Biswal, et al., 2020). Moreover, a network-based study indicated that WM functional connectomes exhibited a stable and reliable small-world topology, offering a neuromarker for MDD-related prognosis and diagnosis (Li, Chen, et al., 2020). All these advances have improved our understanding of the functional information in WM and showed that FC in WM may be a potential approach to investigate behavioral phenotypes in MDD. Newly discovered evidence has revealed that IVFC within WM (WM-IVFC) also exhibits a nonuniform spatial distribution in HCs, similar to GM-IVFC (Li, Wu, et al., 2021). Additionally, the study implied that WM-IVFC might provide complementary functional information for understanding pathophysiology mechanisms of some psychiatric disorders (Li, Wu, et al., 2021). To the best of our knowledge, no study has previously explored whether WM-IVFC is altered in MDD patients, and whether such alteration can provide valuable information for classification and prediction of this disorder.

Many studies indicated that MDD is a moderately heritable disorder (Corfield et al., 2017; Flint & Kendler, 2014; Sullivan et al., 2000). Genome-wide association studies (GWAS) identified several risk genes associated with MDD, some of which play key roles in the biological functions of presynaptic differentiation and neuroinflammation (Howard et al., 2019). Moreover, there is literature that has demonstrated the contribution of genetics to the brain's IVFC (Gao et al., 2014). Recent advances in comprehensive brain-wide gene expression atlases such as the Allen Human Brain Atlas (AHBA) (Hawrylycz et al., 2012) have provided a workable route to linking spatial variations in gene expression to neuroimaging phenotype. By means of this powerful transcription-neuroimaging association

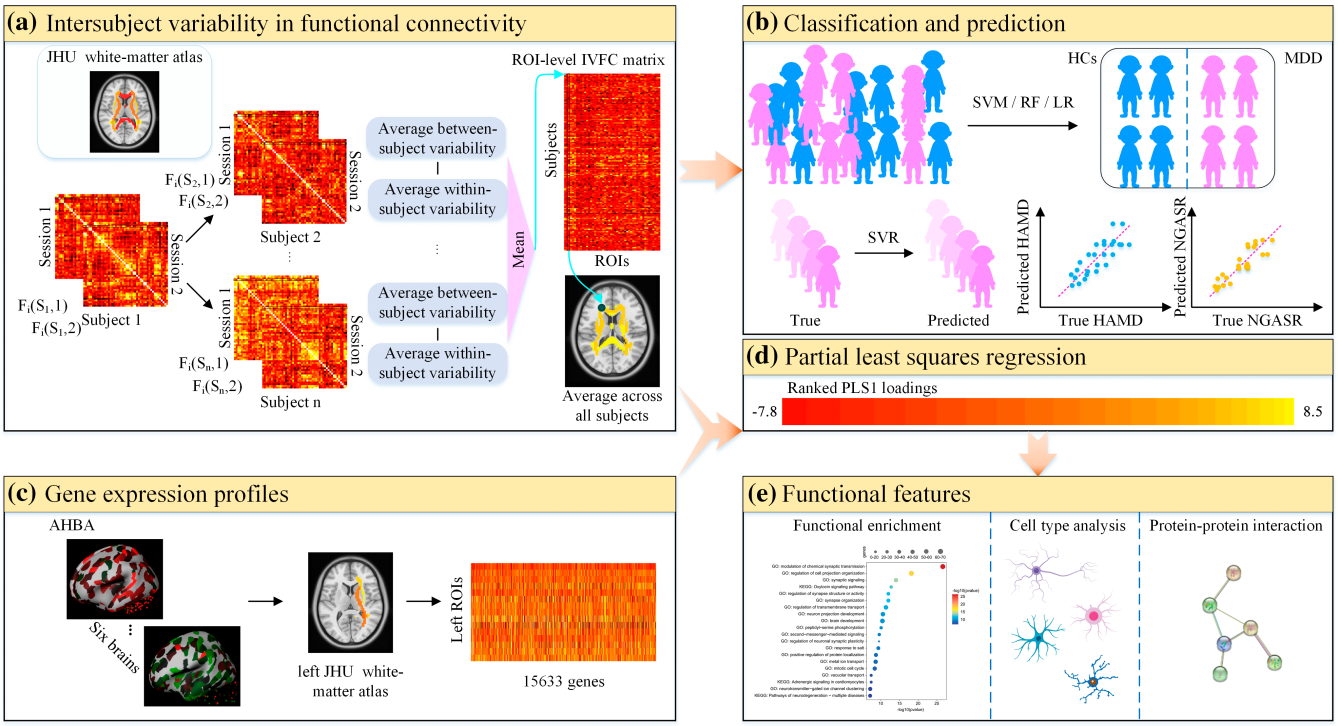

FIGURE 1 Schematic overview of the study design. (a) WM-IVFC calculation. (b) The discriminant WM-IVFC values were used to distinguish MDD patients from HCs and predict depressive severity and suicide risk in patients. (c) Gene expression profiles in WM regions of the left hemisphere were obtained from six postmortem normal brains from AHBA. (d) PLS regression was used to investigate the association between MDD-related WM-IVFC changes and gene expression profiles. (e) A set of analyses were performed to describe functional features of the identified genes. AHBA, Allen human brain atlas; HAMD, Hamilton depression rating scale; IVFC, intersubject variability in functional connectivity; LR, logistic regression; NGASR, Nurses' Global Assessment of Suicide Risk scale; PLS, partial least squares; RF, random forest; SVM, support vector machine; SVR, support vector regression; WM, white-matter.

analysis, researchers have identified several sets of genes whose expression levels are linked to brain structural and functional abnormalities in MDD (Xue et al., 2022) (Li, Seidlitz, et al., 2021). Nonetheless, the molecular genetic underpinnings of WM-IVFC changes in MDD remain unknown.

In the current study, to fill these gaps, we first examined between-group WM-IVFC differences in two independent cohorts and analyzed the behavioral relevance related to the alterations. Next, the discriminant WM-IVFC values were used to classify MDD patients and predict clinical symptoms in patients. In combination with the AHBA, transcriptome-neuroimaging association analyses were further conducted to identify genes whose expression profiles were associated with WM-IVFC changes. Finally, a set of analyses were performed to describe functional features of the identified genes. Schematic overview of the study design is provided in Figure 1.

2 | MATERIALS AND METHODS

2.1 | Participants

The discovery cohort included 145 MDD patients and 119 age- and sex-matched HCs recruited from the Affiliated Yuhuangding Hospital of Qingdao University. The validation cohort included 54 MDD patients and 78 well-matched HCs recruited from the Affiliated Hospital of Binzhou Medical College. Inclusion and exclusion criteria for all participants are described in the Data S1 (Method 1). 24-item Hamilton Depression Rating Scale (HAMD) (Williams, 1988) and Nurses' Global Assessment of Suicide Risk scale (NGASR) (Cutcliffe & Barker, 2004) were applied to capture depression severity and suicide risk in patients. This study was conducted in accordance with the Declaration of Helsinki and was approved by the Ethics Committee of Yantai Yuhuangding Hospital and Affiliated Hospital of Binzhou Medical College. Written informed consent was obtained from all participants.

2.2 | Data acquisition and image preprocessing

All participants in the discovery cohort underwent MRI image scanning using a 3.0T scanner (Discovery 750; GE Healthcare, USA). The MRI data of participants in the validation cohort were collected using a Siemens Skyra 3.0T scanner (Siemens Medical, Erlangen, Germany). Detailed scan sequences and parameters are described in the Data S1 (Method 2). Functional images were preprocessed using DPARSF (v5.2, http://rfmri.org/dparsf) and SPM12 toolbox (http://www.fil.ion.ucl.ac.uk/spm). Slice timing correction and head motion correction were conducted after removing the first 15 time points. Participants

with excessive head motion (2 mm translation or 2.0° rotation) were excluded. Structural images were co-registered to the preprocessed functional images, and then segmented into GM, WM, and cerebrospinal fluid (CSF) by using DARTEL. The resulting images were normalized to the Montreal Neurological Institute space, and each voxel was resampled to $3 \times 3 \times 3$ mm^3. Next, the mean signals from CSF, Friston-24 head motion parameters were regressed out by multiple linear regression analysis. To avoid elimination of important neural signals, we did not remove WM and brain global signal. Finally, smoothing with 6 mm full-width half-maximum, detrending, and temporal filtering (bandpass, 0.01–0.08 Hz) were performed.

2.3 | Construction of WMFC matrix

To construct the brain WMFC matrix, 48 WM regions of interest (ROIs) were initially defined by the JHU ICBM-DTI-81 atlas (Table S1). The time series were then extracted from each ROI by averaging the time series of all voxels within that region. Finally, the Pearson's correlation coefficients between the time series of each pair of ROIs were calculated and normalized using Fisher's z-transformation, resulting in a 48×48 WMFC matrix for each subject.

2.4 | WM-IVFC calculation and group differences

WM-IVFC was estimated in line with a previous study on GM-IVFC (Li, Wei, et al., 2021). The FC profile of each ROI was vectored as $F_i(s,t)$, where $i = 1, 2, \ldots, 48$, the value represented the FC between ROI i and the remaining 47 ROIs; s ($s \in 1, 2, \ldots, n$) denoted the subject, n is the number of subjects in the corresponding group; t ($t \in 1, 2$) denoted the scan session. Specifically, for each subject, all 170 time points were evenly split into two halves (i.e., 1–85 time points for session 1, 86–170 time points for session 2) (Sun et al., 2021). The between-subject variability between subjects s_1 and s_2 for ROI i in each scan session was defined as:

$$R_i(s_1,s_2,t) = 1 - \mathrm{corr}(F_i(s_1,t), F_i(s_2,t))$$

where corr was the function of the Pearson's correlation. The average between-subject variability of subjects s_1 and s_2 across two sessions for ROI i was estimated as:

$$R_i'(s_1,s_2) = \frac{1}{2}[R_i(s_1,s_2,1) + R_i(s_1,s_2,2)]$$

The within-subject variability was measured based on two sessions of a subject. Given an ROI i, the within-subject variability of subject s was defined as:

$$N_i(s) = 1 - corr(F_i(s,1), F_i(s,2))$$

The average within-subject variability of two different subjects s_1 and s_2 for ROI i was estimated as:

$$N_i'(s_1,s_2) = \frac{1}{2}[N_i(s_1) + N_i(s_2)]$$

To estimate the "pure" intersubject variability, the IVFC of ROI i between subjects s_1 and s_2 was estimated by removing the average within-subject variability from the average between-subject variability, that is:

$$IVFC_i(s_1,s_2) = R_i'(s_1,s_2) - N_i'(s_1,s_2)$$

The IVFC of ROI i regarding a single subject s was then calculated as the mean of intersubject variability between s and all other subjects in a group. By averaging intersubject variability across all subjects of each group, the IVFC of ROI i was obtained. Finally, the WM-IVFC map can be obtained for each group.

To estimate significant WM-IVFC changes in MDD, WM-IVFC maps were compared between MDD patients and HCs using a two-sample t test based on each ROI, with gender and age considered as covariates. Subsequently, a statistical t-map was generated. Significance was set at $p < 0.05$ with FDR correction for multiple comparisons. In addition, Pearson's correlation was performed between WM-IVFC values in the significantly altered WM-IVFC regions and clinical variables (HAMD and NGASR scores) in MDD patients.

2.5 | Behavioral relevance analysis

To investigate the behavioral relevance of WM-IVFC changes in MDD, we examined their associations with behavior terms from the NeuroSynth database (http://www.neurosynth.org) (Yarkoni et al., 2011). We used the "decoder" function in Neurosynth to examine the spatial correlations between the t map of WM-IVFC and the meta-analytic map of each term in the database.

2.6 | Classification and prediction of MDD

We distinguished MDD patients from HCs using support vector machine (SVM), random forest (RF), and logistic regression (LR) models. The models were implemented using Machine Learning Toolbox for MATLAB software (version, matlab 2018b; https://www.mathworks.com/products/statistics.html). The discriminant WM-IVFC values were treated as classification features. We used the grid search algorithm to find and determine the optimal parameters of the machine learning algorithm, and the parameters with the highest area under curve (AUC) were selected as the optimal. The optimal parameters (c and gamma) for SVM are 0.5 and 0.25. The models were validated using a 10-fold cross-validation procedure. Basically, all training subjects were partitioned into 10 folds (each fold with a roughly equal sample size), and each time one fold was selected as the testing set, while the remaining nine folds were combined together as the training set. The entire 10-fold cross-validation process was further repeated 10 times. Finally, we reported the average classification results across 100 trials. The classification performance of the models could be

quantified using accuracy, sensitivity, specificity, and AUC of receiver operating characteristic curve (ROC). We also identified features with high discriminative power in three models by examining the weight vectors.

In addition, support vector regression (SVR) models implemented using the MATLAB-based LIBSVM toolbox (v3.5, https://www.csie.ntu.edu.tw/~cjlin/libsvm/) were constructed to predict depression severity and suicide risk in MDD patients. Based on discriminant WM-IVFC values of MDD patients, a grid search algorithm within a 10-fold cross-validation procedure was implemented to automatically identify the optimal parameters for the SVR algorithm. The optimal parameters (c and gamma) for SVR are 1.4 and 5.6. We evaluated the predictive performance by calculating the root mean square error (RMSE) and Pearson correlation between the predicted and actual HAMD and NGASR scores.

2.7 | Gene expression data preprocessing

Brain gene expression data were obtained from the downloadable AHBA dataset (http://human.brain-map.org) (Hawrylycz et al., 2012), which was derived from six postmortem brains (age: 42.50 ± 13.38 years, male/female: 5/1, Table S2). According to the Arnatkevic et al. (Arnatkeviciute et al., 2019), the gene expression data preprocessing steps included: (i) verifying probe-to-gene annotations, (ii) filtering of probes, (iii) probe selection, (iv) sample assignment, (v) normalization of expression measures, and (vi) gene filtering. Since the AHBA dataset only includes the right hemisphere data for two subjects, we only considered the left hemisphere WM regions.

2.8 | Transcription-neuroimaging association analysis

To explore the association between regional WM-IVFC changes (*t*-values from left hemisphere WM regions) and transcriptional activity for all 15,633 genes, a multivariate method called partial least squares (PLS) regression (Krishnan et al., 2011) was used. Gene expression data and regional changes in WM-IVFC were set as predictor variables and response variables, respectively. The first component of the PLS (PLS1) was the linear combination of gene expression values, which was most strongly correlated with regional changes in WM-IVFC. We adopted a spatial autocorrelation corrected permutation test (5000 times) (Vasa et al., 2018) to examine the statistical significance of the variance explained by PLS1. Bootstrapping was used to estimate the error of PLS1 weight estimated for each gene, and the ratio of the weight of each gene to its bootstrap standard error was used to calculate the *Z* scores and sequence the genes according to their contribution to PLS1 (Morgan et al., 2019). The set of genes with an FDR of 5‰, either positive (PLS1+), or negative (PLS1−), constituted the intersubject variability gene list.

To explore the contribution of the MDD-related genes in the PLS analysis, we first obtained the overlapping genes from the 269 MDD-related genes defined by GWAS (Howard et al., 2019) and 15,633 background genes. Then the gene expression levels of these overlapping genes were assessed for correlations with between-group differences in WM-IVFC. FDR < 5% was used to declare significant results for multiple comparisons.

2.9 | Gene functional features

2.9.1 | Functional enrichment

To investigate the biological functions of the genes associated with WM-IVFC changes in MDD, we performed functional enrichment analyses using Metascape (https://metascape.org/gp/index.html#/main/step1). The gene list was analyzed for significant enrichment of gene ontology (GO) biological processes and Kyoto Encyclopedia of Genes and Genomes (KEGG) pathways. The enrichment was thresholded for significance at 5%, corrected by the FDR.

2.9.2 | Cell type analysis

We also explored whether the genes related to WM-IVFC changes in MDD were enriched for specific brain cell types. To obtain gene sets from each cell type, we compiled data from five different single-cell studies using postmortem brain tissue in human postnatal subjects. This approach avoids any deviation from sampling, analysis, or thresholding, leading to the initial inclusion of 58 cell classes. Following the procedure in Seidlitz et al. (Seidlitz et al., 2020), we further divided cell types into seven canonical classes: microglia, endothelial cells, oligodendrocyte precursors, oligodendrocytes. astrocytes, and excitatory and inhibitory neurons. Only one study included the annotation of the Per (pericyte) type, thus this gene set was excluded. Next, we overlapped the gene set of each cell type with the gene list. The *p* value of the number of overlapped genes in each cell type was obtained by a permutation test (5000 times), and corrected by FDR with $p < 0.05$.

2.9.3 | Protein–protein interaction

Protein–protein interaction (PPI) analysis was conducted with STRING v11.0 (https://string-db.org/) to examine whether the genes associated with WM-IVFC changes in MDD could construct a PPI network with a highest confidence interaction score of 0.9. The top 10% genes were defined as hub genes by using the degree and MCC algorithms of the Cytoscape.

2.10 | Validation analysis

The above between-group differences in WM-IVFC were examined in the validation cohort. Pearson correlation analysis was conducted to examine the similarity between the *t* map from the discovery cohort and the identically derived *t* map from the validation cohort. To further externally validate the generalization of the classification models

using SVM, RF, LR, and the predictive model, the models trained using the discover cohort were applied to the validation cohort directly.

For validating the identified genes associated with WM-IVFC changes in MDD, a multigene-list meta-analysis was performed between the gene lists of the discovery and validation cohorts. The set of genes with an FDR of 5‰ was significant in the validation cohort. The degree of gene overlap was evaluated by the odds ratio (OR).

3 | RESULTS

3.1 | Demographic and clinical characteristics

The demographic and clinical characteristics of the discovery and validation cohorts are shown in Table 1. No significant differences were found in gender, age, body mass index, and education between MDD and HCs ($p = 0.323$, 0.207, 0.215, and 0.127). MDD patients obtained significantly higher HAMD scores than HCs ($p < 0.05$).

3.2 | WM-IVFC changes in MDD patients

The regional two-sample t test revealed a mix of increased and decreased WM-IVFC in MDD patients (Figure 2 and Table 2). Specifically, MDD patients showed significantly increased IVFC in the genu of corpus callosum, right anterior corona radiata, left superior corona radiata, left external capsule, right cingulum hippocampus, right sagittal stratum, right superior longitudinal fasciculus, bilateral superior fronto-occipital fasciculus, and left uncinate fasciculus relative to HCs ($p_{FDR} < 0.05$). In addition, MDD patients showed significantly decreased IVFC in the left corticospinal tract, left inferior cerebellar peduncle, right superior cerebellar peduncle, bilateral cerebral peduncle, right anterior limb of internal capsule, and left posterior limb of internal capsule in comparison with HCs ($p_{FDR} < 0.05$). We found that there was a significantly positive correlation between WM-IVFC values and HAMD scores in the right superior fronto-occipital fasciculus of MDD patients ($r = 0.395$, $p = 0.019$; Figure S1). However, no significant correlations (all $p > 0.05$) were found between WM-IVFC values and NGASR scores in MDD patients.

3.3 | Behavioral relevance

The MDD-related WM-IVFC changes were correlated with multiple behavioral terms mainly involved in sensorimotor processes, including "visual", "motor" and "sensory", as well as higher-order functions, such as "working memory", "learning task", "execution", "motor imagery", "emotion", and "language" (Figure 3a).

3.4 | Classification and prediction of MDD

The classification models achieved excellent performance with the AUC of 0.889, 0.901, 0.897; accuracy of 0.870, 0.852, 0.833; sensitivity of 0.900, 0.867, 0.767; specificity of 0.833, 0.833, 0.917 for SVM, RF, and LR classifiers, respectively. Classification performance of the three models is given in Figure 3b and Table S3. Then we summarized the top 10 features with the highest discriminative power in three models, and six of these features overlapped, as shown in Table S4.

Additionally, the predictive model showed a significant correlation between the observed and predicted HAMD scores (RMSE = 0.033, $r = 0.575$, $p = 0.002$; Figure 3c). And a significant correlation between the observed and predicted NGASR scores (RMSE = 0.036, $r = 0.384$, $p = 0.040$; Figure 3d) was also found. The results imply that the discriminant WM-IVFC of MDD patients could predict depression severity and suicide risk.

3.5 | Gene expression related to WM-IVFC changes in MDD patients

The PLS1 component accounting for approximately 59.4% of the variance was statistically significant (p_{spin} <0.001, the permutation test

TABLE 1 Demographic and clinical characteristics (mean ± SD).

	Discovery cohort			Validation cohort		
Characteristics	MDD ($n = 145$)	HCs ($n = 119$)	p value	MDD ($n = 54$)	HCs ($n = 78$)	p value
Gender (male/female)	46/99	37/82	0.323	18/36	29/49	0.495
Age (years)	37.54 ± 12.93	34.68 ± 11.54	0.207	43.73 ± 10.07	45.61 ± 8.40	0.362
Race	Chinese	Chinese		Chinese	Chinese	
BMI	21.87 ± 3.76	23.91 ± 3.95	0.215	24.12 ± 3.52	23.87 ± 3.44	0.289
Education (years)	10.18 ± 3.78	11.79 ± 3.21	0.127	11.84 ± 2.93	12.13 ± 3.17	0.192
Duration of illness (months)	21.13 ± 27.06	NA		12.32 ± 15.96	NA	
HAMD-24	32.09 ± 12.60	4.24 ± 3.72	<0.001	30.86 ± 11.52	2.24 ± 3.32	<0.001
NGASR	8.97 ± 1.88	NA		NA	NA	

Abbreviations: BMI, body mass index; HAMD, Hamilton depression rating scale; HCs, healthy controls; MDD, major depression disorder; NA, not available; NGASR, Nurses' Global Assessment of Suicide Risk scale.

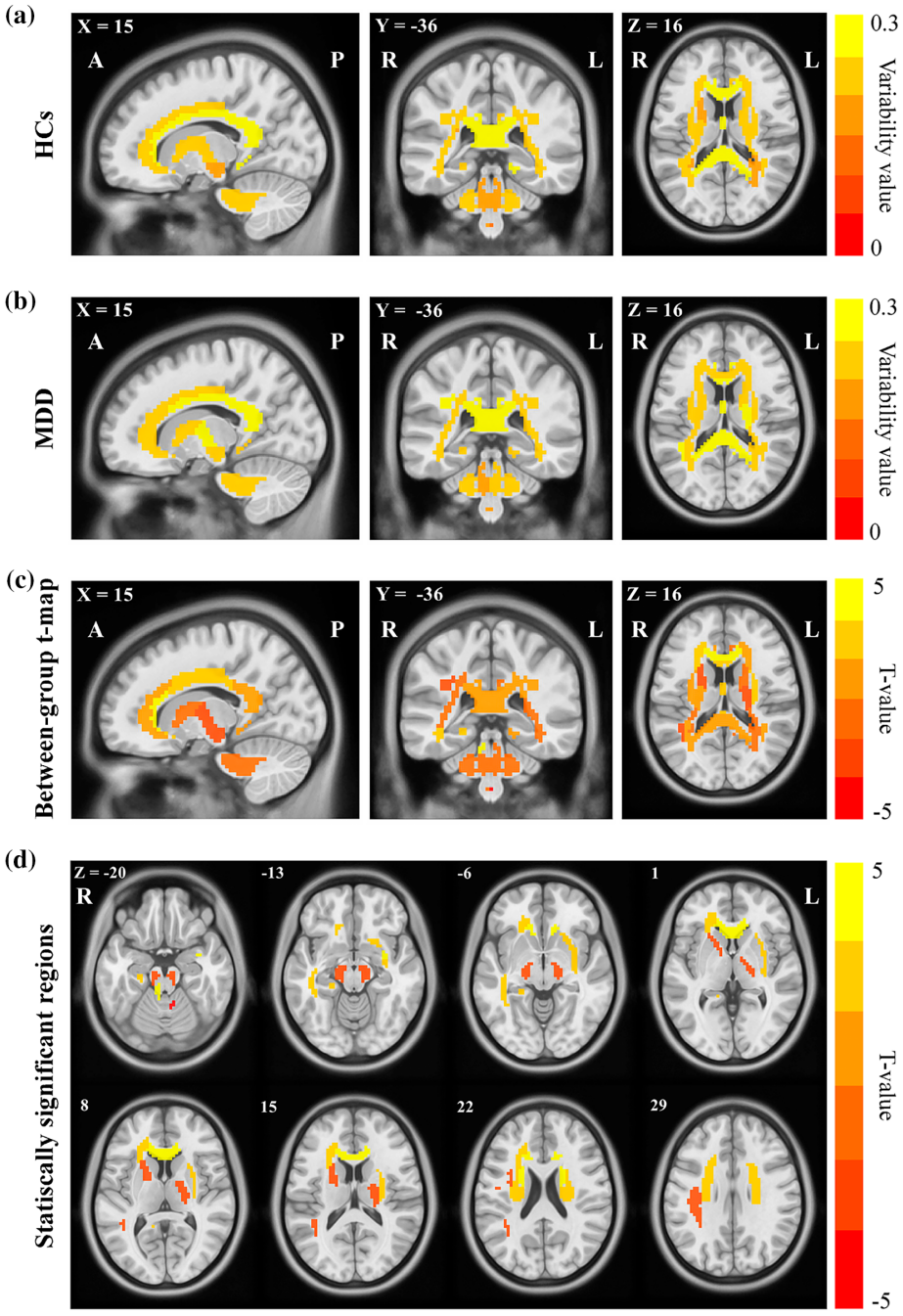

FIGURE 2 Group differences of WM-IVFC. (a) WM-IVFC map in HCs; (b) WM-IVFC map in MDD; (c) Between-group comparison (*t*-map) of regional WM-IVFC (uncorrected); (d) WM regions showed statistically significant differences ($p_{FDR} < 0.05$). IVFC, intersubject variability in functional connectivity; WM, white matter.

randomly "spins" the *t* map). As shown in Figure 4b, the distribution of the PLS1 scores revealed a regional variation in the transcriptional architecture of human WM. And PLS1 scores were positively correlated with the between-group *t* map ($r = 0.770$, $p_{spin} < 0.001$; Figure 4c). We found 1004 genes comprised the regional changes in WM-IVFC gene list, including 787 PLS1+ ($Z > 5$) and 217 PLS1− ($Z < -5$) genes (all $p_{FDR} < 0.005$; Figure 4d). We then selected 221 genes by overlapping 269 MDD-related genes defined by GWAS with the 15,633 background genes. Transcriptional correlation with WM-IVFC changes was significantly correlated with 69 of 221 genes (all $p_{FDR} < 0.05$; Figure 4e and Table S5), including 51 positive correlations and 18 negative correlations. The gene with the highest positive weight was AREL1 ($r = 0.761$, $p = 0.001$). The gene with the lowest negative weight was FHIT ($r = -0.654$, $p = 0.008$; Figure 4f).

3.6 | Gene functional features

The top 20 significant pathways were identified. With regard to GO, we found the variability-related genes were significantly enriched for biological processes associated with synapse (modulation of chemical synaptic transmission, synaptic signaling, regulation of synapse structure or activity, synaptic organization), nervous system (neuron projection development, brain development, regulation of neuronal

TABLE 2 WM regions showed statistically significant differences ($p_{FDR} < 0.05$).

WM ROIs	Abbreviation	R/L	*t* value	*p* value
MDD > HC				
Genu of corpus callosum	GCC		4.137	1.061×10^{-4}
Anterior corona radiata	ACR	R	2.504	0.0029
Superior corona radiata	SCR	L	2.213	0.0041
Sagittal stratum (include inferior longitudinal fasciculus and fronto-occipital fasciculus)	SS	R	1.987	0.0067
External capsule	EC	L	2.390	0.0036
Cingulum (hippocampus)	CGH	R	2.358	0.0036
Superior longitudinal fasciculus	SLF	R	2.549	0.0028
Superior fronto-occipital fasciculus	SFO	R	2.617	0.0026
Superior fronto-occipital fasciculus	SFO	L	3.258	7.115×10^{-4}
Uncinate fasciculus	UF	L	2.702	0.0023
MDD < HC				
Corticospinal tract	CST	L	−3.671	2.815×10^{-4}
Inferior cerebellar peduncle	ICP	L	−4.098	6.239×10^{-4}
Superior cerebellar peduncle	SCP	R	−2.833	0.0019
Cerebral peduncle	CP	R	−2.347	0.0034
Cerebral peduncle	CP	L	−3.119	9.024×10^{-4}
Anterior limb of internal capsule	ALIP	R	−2.231	0.0042
Posterior limb of internal capsule	PLIC	L	−1.977	0.0065

synaptic plasticity), and ion channel (metal ion transport, neurotransmitter-gated ion channel clustering). There were also significantly enriched KEGG pathways, such as Oxytocin signaling pathway. The results of functional enrichment are provided in Figure 5a and Table S6.

Cell type analysis revealed that the variability-related genes were primarily expressed in neurons, both excitatory (176 genes, adjusted $p_{perm} < 2.803 \times 10^{-4}$, FDR-corrected) and inhibitory (97 genes, adjusted $p_{perm} = 0.0048$, FDR-corrected). The corresponding results are illustrated in Figure 5b.

PPI analysis revealed that the variability-related genes could construct an interconnected PPI network (Figure 5c). The resulting network had 952 connected proteins and 472 edges, significantly more than the 301 edges expected by chance ($p < 10^{-16}$). Moreover, we identified 20 hub genes based on the degree and MCC algorithms (Figure 5d and Table S8). Notably, nine genes were found to overlap between the two methods.

3.7 | Reproducibility of WM-IVFC changes in MDD and transcriptomic profiles

Many WM regions with significant differences determined by using discovery cohort still exhibit significant differences between patients and control groups in the validation cohort (Figure 6a). The between-group *t*-map from the validation cohort was positively correlated to the discovery cohort ($r = 0.336$, $p = 0.019$; Figure 6b). The classification models achieved good performance in the validation cohort, with the AUC of 0.877, 0.886, and 0.877 for SVM, RF, and LR classifiers, respectively (Figure 6c and Table S3). The predictive model showed a significant correlation between the observed and predicted HAMD scores in the validation cohort (RMSE = 0.003, $r = 0.362$, $p = 0.032$; Figure 6d).

In the validation cohort, we found that 532 PLS1+ and 83 PLS− genes (all $p_{FDR} < 0.005$) were significantly overexpressed in WM regions, consisting of 615 regional WM-IVFC gene list differences. There was a significant overlap between the gene lists in the discovery and validation cohorts: OR = 35.4, $p < 0.0001$ (Figure 6e). We also identified several overlapped enrichment pathways between the discovery and replication cohorts, including "modulation of chemical synaptic transmission", "synapse organization", "regulation of synapse organization", "brain development", and "second-messenger-mediated signaling" (Figure 6f, g). This supports the generalized relationship between gene expression and the MDD-related WM-IVFC changes.

4 | DISCUSSION

To our knowledge, this study is among the first to report altered inter-subject functional variability of brain WM in MDD and its association with transcriptional profiles. Here we uncovered extensive WM-IVFC alterations in MDD compared to HCs, which were associated with domains involving sensorimotor processes and higher-order cognition. Moreover, the discriminant WM-IVFC could be utilized to distinguish MDD patients from HCs and predict the depression severity and

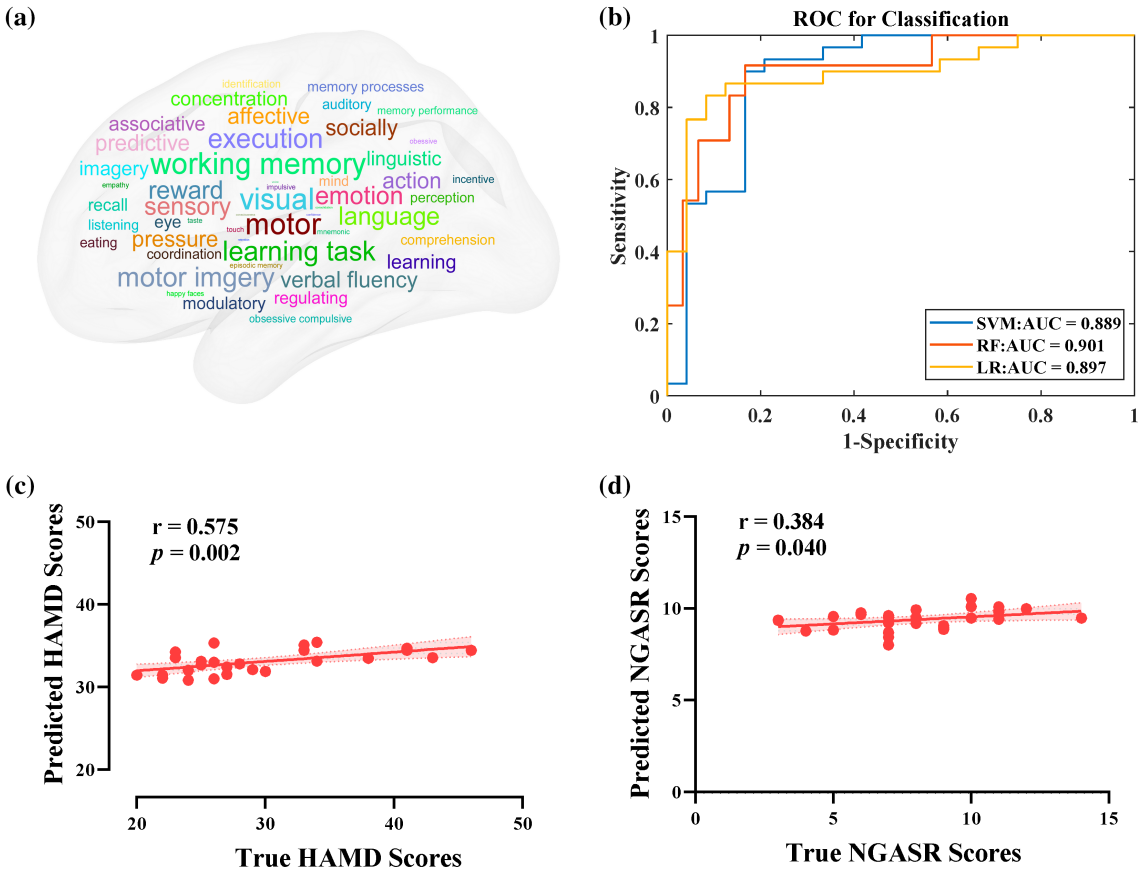

FIGURE 3 The clinical relevance of WM-IVFC changes in MDD. (a) Distribution of behavior terms correlated with MDD-related WM-IVFC changes. (b) ROC curves of the models based on altered regional WM-IVFC using SVM, RF, and LR classifiers. (c) Prediction of depression severity based on altered regional WM-IVFC in MDD patients. (d) Prediction of suicide risk based on altered regional WM-IVFC in MDD patients. AUC, area under curve; HAMD, Hamilton depression rating scale; LR, logistic regression; NGASR, Nurses' global assessment of suicide risk scale; RF, random forest; ROC, receiver operator characteristic; SVM, support vector machine; SVR, support vector regression.

suicide risk in patients. Further transcriptome-neuroimaging correlation analysis revealed that the variability-related genes were enriched for synapse, neuronal system, and ion channel, and predominantly expressed in excitatory and inhibitory neurons. We demonstrated the generalizability of our results in an independent cohort. Our findings provided potential implications for understanding clinical heterogeneity of MDD.

4.1 | MDD-related WM-IVFC alterations

In the present study, MDD patients showed increased IVFC in multiple WM regions. These altered regions are consistent with those reported in previous studies based on other technologies. The corpus callosum, as the largest interhemispheric commissure in the human brain, connects the anterior cingulate cortex and orbitofrontal cortex of the two hemispheres (Roland et al., 2017). It is generally believed that corpus callosum abnormalities underlie many of the emotional, cognitive and behavioral deficits in MDD (Koshiyama, Fukunaga, Okada, Morita, Nemoto, Usui, & Cocoro., 2020). The superior longitudinal fasciculus, inferior longitudinal fasciculus, and fronto-occipital fasciculus belong to long contact tracts, which are connected with the cortex of the ipsilateral hemisphere (Schmahmann et al., 2007). They play important roles in cognitive function, visual spatial processing, object recognition and memory (Koshiyama, Fukunaga, Okada, Morita, Nemoto, Yamashita, & Hashimoto, 2020; Thomas et al., 2009). Reduced fractional anisotropy (FA) and disruptions in WM integrity in these structures have been reported in MDD (Cole et al., 2012; de Diego-Adelino et al., 2014). It has been shown that cingulum participates in working memory functioning and diffusion MRI studies have revealed that FA at cingulum hippocampus decreased in MDD compared to HCs (Bubb et al., 2018; Korgaonkar et al., 2014). Aberrant microstructure of the uncinate fasciculus, a WM tract implicated in emotion regulation, has been hypothesized as a neurobiological mechanism of MDD (Xu et al., 2023). In our study, increased intersubject functional variability was observed in uncinate fasciculus and corona radiata, which extend previous findings that the microstructure of these tracts may be significant neural indicators of individual differences in cognitive domains including emotion and attention (Niogi et al., 2010; Pedersen et al., 2022). Our study also supports the role of the abnormal external capsule in MDD as previously described (Cole et al., 2012). Greater IVFC of these WM regions could partially explain high heterogeneity of clinical symptoms and the diverse dysconnectivity observed across studies in MDD. A previous study showed that

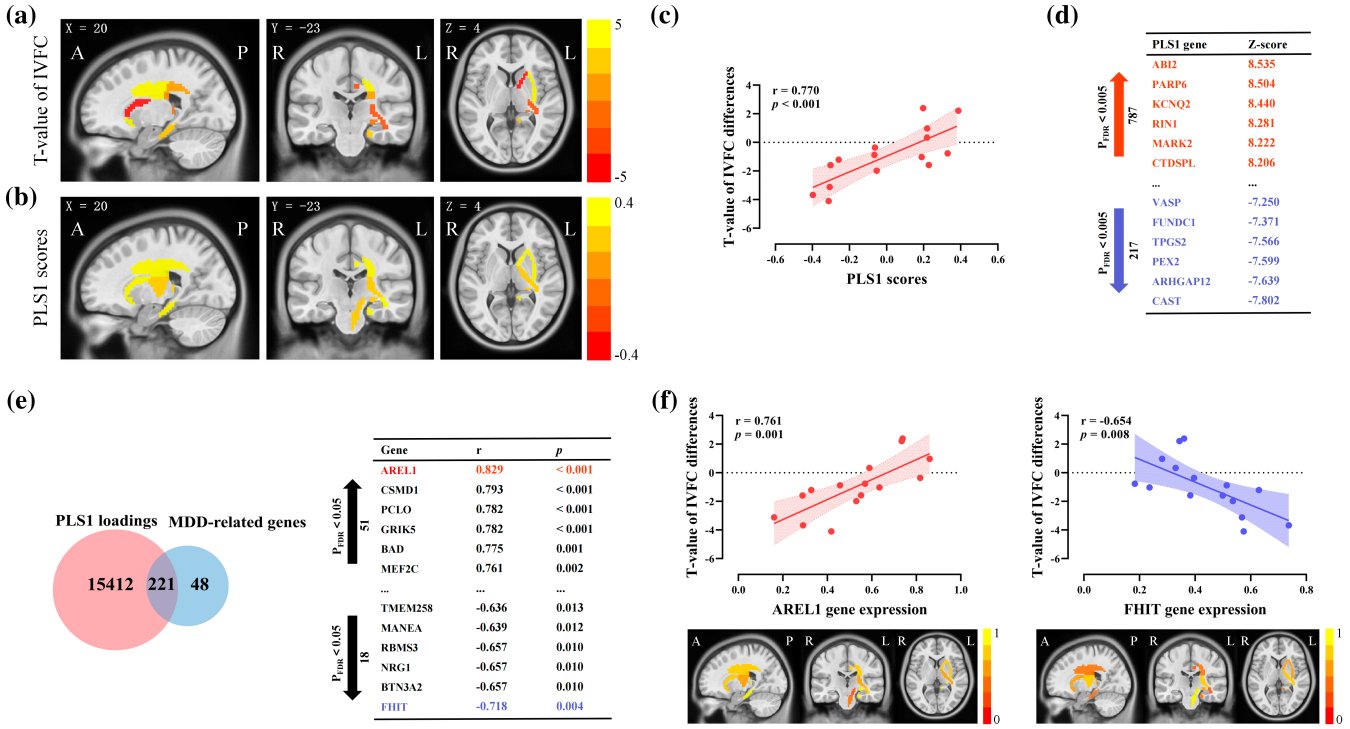

FIGURE 4 Gene expression profiles related to WM-IVFC changes in MDD. (a) WM-IVFC differences between MDD and HCs in the left hemisphere (uncorrected). (b) Weighted gene expression map of PLS1 scores in the left hemisphere. (c) Scatterplot of PLS1 scores (weighted sum of 15,633 gene expression value in left WM regions) versus between-group differences in WM-IVFC. (d) Ranked PLS1 loadings. (e) MDD-related genes expression profiles from GWAS correlated with WM-IVFC differences. Overlapped genes between GWAS and 15,633 background genes. (f) Genes that are strongly correlated with between-group differences in WM-IVFC. GWAS, genome-wide association studies; IVFC, intersubject variability in functional connectivity; WM, white matter.

intersubject functional variability was widely increased in brain GM of MDD patients, which was correlated with individual behavioral differences (Hou et al., 2023). Our study enhances current knowledge by offering unique insight into functional variability of brain WM. In addition, the study also showed that IVFC in some WM regions was decreased in MDD. Generally, corticospinal tract, cerebellar peduncle, cerebral peduncle and internal capsule are thought to communicate motor-related information (Lemon, 2008). Damage to the internal capsule is closely related to motor and sensory dysfunction in MDD (E. V. Sullivan et al., 2010). We speculate that decreased IVFC in these WM tracts may be indicative of MDD-related behavioral changes, such as motor retardation (Shaffer et al., 2022). Collectively, our findings have provided preliminary evidence of WM-IVFC alterations in MDD patients.

4.2 | Clinical significance of WM-IVFC alterations

The correlation results showed that when the WM-IVFC value of right superior fronto-occipital fasciculus in MDD increased, the depression symptom aggravated. Some studies reported that fronto-occipital fasciculus plays a vital role in depression (Manelis et al., 2021). Unexpectedly, we did not find any significant correlations between WM-IVFC values and NGASR scores in MDD patients. The reasons for the non-significant findings are elusive, but they may be related to the relatively small sample size, the clinical features of patients (first-episode, treatment-naïve), and others. Regarding behavioral relevance, our meta-analysis confirmed that MDD-related changes in WM-IVFC were associated with multiple behavioral domains, including sensorimotor processes and higher-order functions. Echoing this finding, deficits in these behavioral domains have been widely reported in MDD (Bubl et al., 2010; Dillon & Pizzagalli, 2018; Millan et al., 2012). We further conducted additional exploratory analyses to investigate the potential clinical significance of WM-IVFC. For classification application, the discriminant WM-IVFC could be utilized to effectively distinguish MDD patients from HCs. Previous literature has suggested that WM functional topology could serve as a neuromarker for MDD classification (Li, Chen, et al., 2020). Our results further contribute to the understanding of the importance of functional organization within WM for the diagnosis of MDD. And the models using SVM, RF, and LR classifiers all achieved commendable classification performance. This implies that our findings remain unaffected by the choice of classifier. Notably, the IVFC of the corpus callosum contributed greatly to MDD classification in three models, which is consistent with reports suggesting that the corpus callosum appears to be consistently more affected in MDD (Won et al., 2016). Our findings, along with other studies, demonstrated that both structural and functional alterations of corpus callosum can distinguish MDD patients from HCs (Matsuoka et al., 2017). For prediction application, apart from predicting depression severity, altered regional WM-IVFC showed potential value in

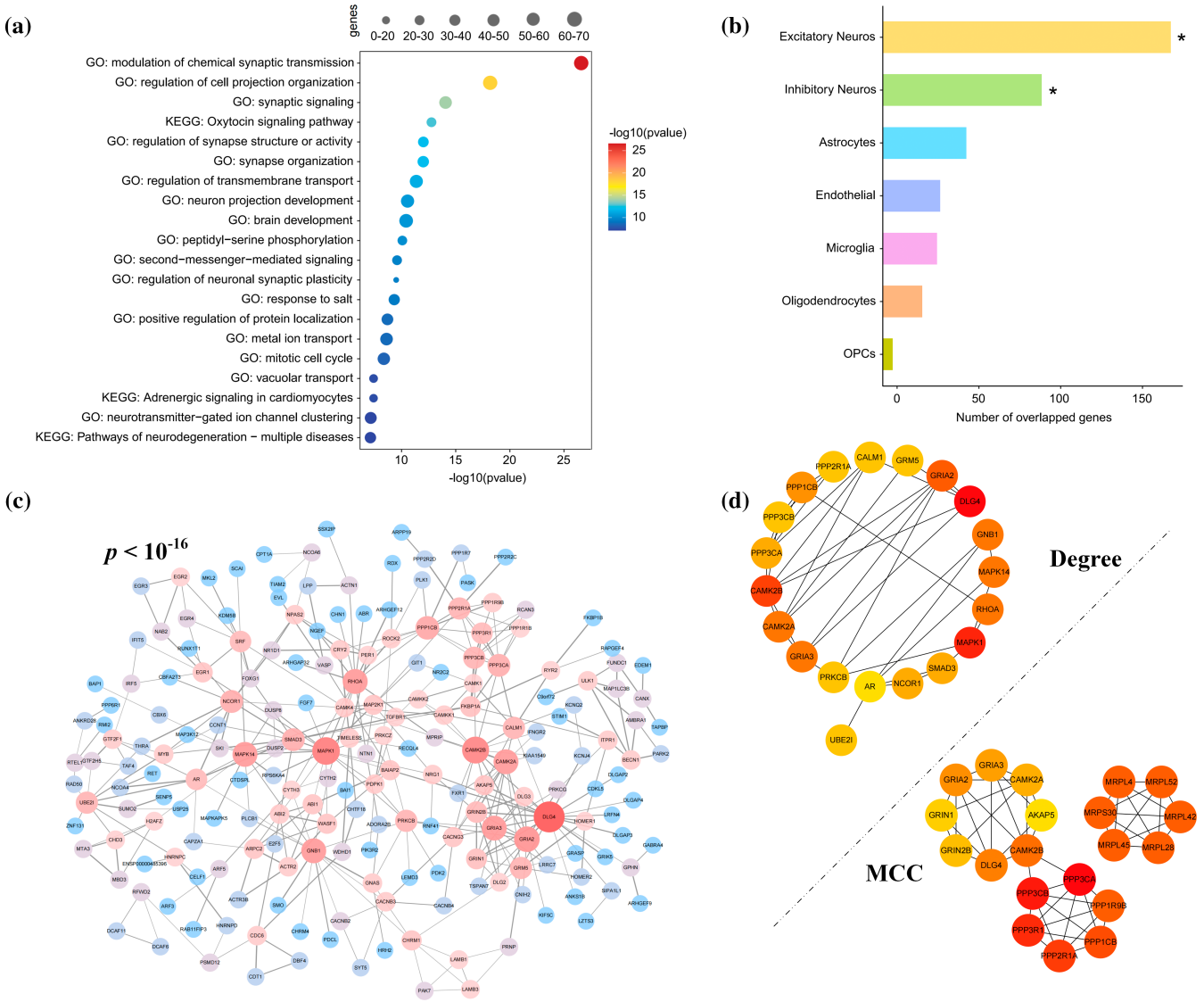

FIGURE 5 A set of analyses on the genes related to WM-IVFC changes in MDD. (a) Ontology terms for variability-related genes (p_{FDR} <0.05). The size of the circle represents the number of genes involved in a given term. (b) Overlapping gene numbers of variability-related genes in each cell types (p_{FDR} <0.05). (c) A PPI network with statistical significance was constructed by variability-related genes. (d) 20 hub genes based on the degree and MCC algorithms in the PPI network. GO, gene ontology; KEGG, Kyoto Encyclopedia of Genes and Genomes; OPC, oligodendrocyte precursors; PPI, protein–protein interaction. The asterisk indicates significance found.

predicting suicide risk in individuals with MDD. Suicide is the most serious consequence of depression (Kessler et al., 2005). There is a particularly high incidence of suicide among MDD patients, leading to a substantial increase in the economic burden nationwide (Ma et al., 2019). Thus, conducting screening for suicide attempts holds immense significance.

4.3 | Gene expression profiles related to WM-IVFC alterations

MDD-related changes in WM-IVFC may be attributed to various factors, including genetic, molecular, and neuronal alterations. The positive correlation between PLS1 scores and the between-group *t* map means that positively weighted genes were overexpressed in WM regions where IVFC was increased in MDD, while negatively weighted genes were overexpressed in WM regions where IVFC was decreased in MDD. Further overlapped gene correlation analysis suggested that AREL1 was the strongest positively correlated gene, with FHIT showing the strongest negatively association. The AREL1 gene codes for an E3 ubiquitin ligase involved in protein ubiquitination and degradation. Intriguingly, β-Arrestins undergo post-translational modification through ubiquitination and are suggested to play a role in the pathophysiology of depression and in the mechanism of antidepressant action (Golan et al., 2013). FHIT plays an important role in systemic oxidatively generated DNA/RNA damage

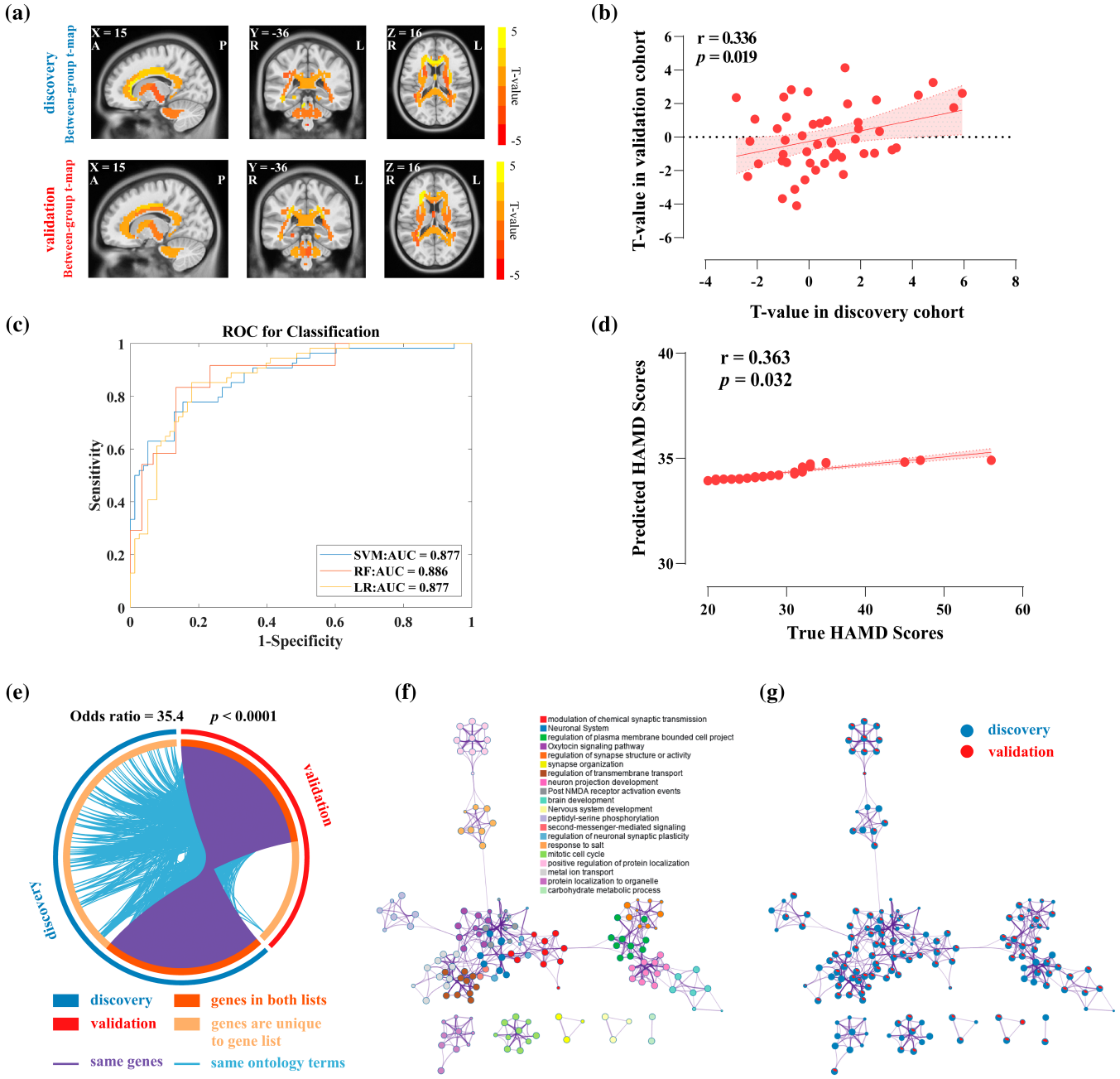

FIGURE 6 Reproducibility of WM-IVFC changes in MDD and transcriptomic profiles. (a) Regional between-group WM-IVFC differences in validation cohort. (b) Pearson's correlation analysis for *t*-values between discovery and validation cohorts ($r = 0.336$, $p = 0.019$). (c) ROC curves of the models using SVM, RF, and LR classifiers in the validation cohort. (d) Prediction of depression severity of MDD patients in the validation cohort. (e) Circos plot of genes overlapped between discovery and validation cohorts. (f) A subset of representative terms from all clusters. (g) The same enrichment network with its nodes displayed as pie sections. Each pie sector is proportional to the number of hits originating from a gene list. AUC, area under curve; HAMD, Hamilton Depression Rating Scale; LR, logistic regression; NGASR, Nurses' Global Assessment of Suicide Risk scale; RF, random forest; ROC, receiver operator characteristic; SVM, support vector machine; SVR, support vector regression.

(Karras et al., 2014), which is linked to depression severity in individuals with MDD (Jorgensen et al., 2013). It is a circadian clock modification gene and related to daytime sleepiness (Gottlieb et al., 2007), potentially contributing to the development of MDD. Our findings demonstrate the genetic association with WM-IVFC phenotypes.

4.4 | Functional features of variability-related genes

Enrichment analyses showed that the identified variability-related genes were significantly enriched for synapse, neuronal system and ion channel. It is widely believed that brain function relies on the abil-

ity of neurons to communicate with each other and that inter-neuronal communication primarily depends on synapses (de Wit & Ghosh, 2016). Basic studies have shown that ketamine, a rapid antidepressant, can reverse the effects of stress and depression on synapse function and generate new synapses in stress-sensitive brain regions (Duman & Aghajanian, 2012). Neurons are a main component of the neurovascular unit. Neurovascular interactions are crucial for maintaining homeostasis of the brain internal environment and contribute to normal brain development (Iadecola, 2017). There is growing evidence of neurovascular coupling disruption in major psychiatric disorders, including MDD (Segarra et al., 2019). Ion channels are important mediators of physiological functions in the central nervous system, influencing neuronal activity, signal transduction, and neurotransmitter release (Kumar et al., 2016). Ion channels, such as low-voltage-sensitive T-type calcium channel inhibitor and potassium channel Kir4.1 inhibitor have been reported to hold promise as therapeutic targets for depression (Hashimoto, 2019). The identified KEGG pathways also have MDD-related biological annotations. Oxytocin-mediated synaptic plasticity in the nucleus accumbens establishes a critical period for social reward learning (Nardou et al., 2019), which have implications for understanding the pathogenesis of social dysfunction in MDD. Our findings not only contribute to a better understanding of the molecular basis of WM-IVFC changes in MDD, but hold the value for clinical translation.

The study showed that the cellular organization of the human brain provides a biological mechanism capable of translating MDD-related WM-IVFC changes into specific cell types alterations. Our results showed variability-related genes were specifically expressed in excitatory and inhibitory neurons, which was consistent with the previous single-cell gene expression study in MDD (Nagy et al., 2020). In recent years, the target cell types in MDD pathophysiology have expanded from excitatory neurons to inhibitory interneurons (Northoff & Sibille, 2014). Considering the crucial role that the balance between excitatory and inhibitory neurons plays in information processing and high-order cognitive functions (Fee et al., 2017), an imbalance between the two may contribute to MDD.

Of note, the genes associated with WM-IVFC alterations in MDD could construct an interconnected PPI network. The hub genes identified by the degree and MCC algorithms showed significant overlap, which hold important functional significance for the pathology and treatment of MDD. For example, the Dlg4 gene encodes for post-synaptic density protein 95 (PSD95), a major synaptic protein that clusters glutamate receptors and is critical for plasticity (Bustos et al., 2017). PSD95 is considered to be implicated in MDD and several novel antidepressants targeting glutamate receptors have been developed (Dean et al., 2021). The validation of the gene set obtained from WM-IVFC changes was further confirmed by this information.

4.5 | Limitations

This study has limitations. First, we only uncovered the WM-IVFC changes in MDD from the brain region level. And its changes should be analyzed from multiple scales including voxels and networks in the future. Second, we calculated WM-IVFC by splitting the time series into the first and the second halves in this study. The R-fMRI data should be collected in two sessions on two different days to validate the replicability of the findings. Third, the gene expression data and neuroimaging data were not collected from the same participants, and were susceptible to intersubject variability. Fourth, the AHBA only included data for the right hemisphere of two participants. Thus, the relationship between genes and MDD-related WM-IVFC changes does not represent the condition of the entire brain. Further studies on relating gene expression profiles to bilateral WM-IVFC alterations in MDD by leveraging transcriptional data from the AHBA and weighted gene co-expression network analysis (Xue et al., 2022) are expected. Fifth, as there were no NAGSA scores available for MDD patients in the validation cohort, we were unable to validate this finding. Future research should test the reproducibility of this finding on an independent, large cohort of participants. Finally, IVFC between brain regions is thought to result from gene–environment interaction. The influence of environmental factors on the heterogeneity of brain function and clinical manifestations in MDD should be investigated in the future.

5 | CONCLUSIONS

In conclusion, we uncovered widely altered WM-IVFC in MDD, which showed strong behavioral relevance and could be used as a potential biomarker for classification and prediction of this disorder. We further linked WM-IVFC phenotypes to gene expression levels. This study offered unique insight into intersubject functional variability of brain WM, promoting an integrative understanding of clinical heterogeneous in MDD.

AUTHOR CONTRIBUTIONS

Qun Gai, Tongpeng Chu, Ning Mao, and Haizhu Xie designed research; Qun Gai, Qinghe Li, Yuting Guo, Heng Ma, Yinghong Shi, Kaili Che, Feng Zhao, Fanghui Dong, and Yuna Li collected data; Qun Gai, Tongpeng Chu, Qinghe Li, Yuting Guo and Haizhu Xie performed data quality control; Qun Gai and Tongpeng Chu analyzed data; Qun Gai, Tongpeng Chu, and Ning Mao wrote the article.

ACKNOWLEDGEMENTS

This study was supported by National Natural Science Foundation of China (82371933, 62176140), Natural Science Foundation of Shandong Province (ZR2023QH084, ZR2023QH107) and Taishan Scholar Foundation of Shandong Province of China (tsqn202211378).

CONFLICT OF INTEREST STATEMENT

The authors declare that they have no conflict of interest.

DATA AVAILABILITY STATEMENT

The Allen Human Brain microarray dataset is available at http://www.human.brain-map.org. The data that support the findings of this study are available from the corresponding author, upon reasonable request.

ORCID

Tongpeng Chu https://orcid.org/0000-0002-6854-4149

Haizhu Xie https://orcid.org/0000-0002-5962-3558

REFERENCES

Arnatkeviciute, A., Fulcher, B. D., & Fornito, A. (2019). A practical guide to linking brain-wide gene expression and neuroimaging data. *NeuroImage*, *189*, 353–367. https://doi.org/10.1016/j.neuroimage.2019.01.011

Biswal, B., Yetkin, F. Z., Haughton, V. M., & Hyde, J. S. (1995). Functional connectivity in the motor cortex of resting human brain using echo-planar MRI. *Magnetic Resonance in Medicine*, *34*(4), 537–541. https://doi.org/10.1002/mrm.1910340409

Bubb, E. J., Metzler-Baddeley, C., & Aggleton, J. P. (2018). The cingulum bundle: Anatomy, function, and dysfunction. *Neuroscience and Biobehavioral Reviews*, *92*, 104–127. https://doi.org/10.1016/j.neubiorev.2018.05.008

Bubl, E., Kern, E., Ebert, D., Bach, M., & Tebartz van Elst, L. (2010). Seeing gray when feeling blue? Depression can be measured in the eye of the diseased. *Biological Psychiatry*, *68*(2), 205–208. https://doi.org/10.1016/j.biopsych.2010.02.009

Bustos, F. J., Ampuero, E., Jury, N., Aguilar, R., Falahi, F., Toledo, J., Ahumada, J., Lata, J., Cubillos, P., Henríquez, B., Guerra, M. V., Stehberg, J., Neve, R. L., Inestrosa, N. C., Wyneken, U., Fuenzalida, M., Härtel, S., Sena-Esteves, M., Varela-Nallar, L., … van Zundert, B. (2017). Epigenetic editing of the Dlg4/PSD95 gene improves cognition in aged and Alzheimer's disease mice. *Brain*, *140*(12), 3252–3268. https://doi.org/10.1093/brain/awx272

Cole, J., Chaddock, C. A., Farmer, A. E., Aitchison, K. J., Simmons, A., McGuffin, P., & Fu, C. H. (2012). White matter abnormalities and illness severity in major depressive disorder. *The British Journal of Psychiatry*, *201*(1), 33–39. https://doi.org/10.1192/bjp.bp.111.100594

Corfield, E. C., Yang, Y., Martin, N. G., & Nyholt, D. R. (2017). A continuum of genetic liability for minor and major depression. *Translational Psychiatry*, *7*(5), e1131. https://doi.org/10.1038/tp.2017.99

Cutcliffe, J. R., & Barker, P. (2004). The Nurses' global assessment of suicide risk (NGASR): Developing a tool for clinical practice. *Journal of Psychiatric and Mental Health Nursing*, *11*(4), 393–400. https://doi.org/10.1111/j.1365-2850.2003.00721.x

DALYs, G. B. D., & Collaborators, H. (2018). Global, regional, and national disability-adjusted life-years (DALYs) for 359 diseases and injuries and healthy life expectancy (HALE) for 195 countries and territories, 1990-2017: A systematic analysis for the global burden of disease study 2017. *Lancet*, *392*(10159), 1859–1922. https://doi.org/10.1016/S0140-6736(18)32335-3

de Diego-Adelino, J., Pires, P., Gomez-Anson, B., Serra-Blasco, M., Vives-Gilabert, Y., Puigdemont, D., Martín-Blanco, A., Alvarez, E., Pérez, V., & Portella, M. J. (2014). Microstructural white-matter abnormalities associated with treatment resistance, severity and duration of illness in major depression. *Psychological Medicine*, *44*(6), 1171–1182. https://doi.org/10.1017/S003329171300158X

de Wit, J., & Ghosh, A. (2016). Specification of synaptic connectivity by cell surface interactions. *Nature Reviews. Neuroscience*, *17*(1), 22–35. https://doi.org/10.1038/nrn.2015.3

Dean, R. L., Hurducas, C., Hawton, K., Spyridi, S., Cowen, P. J., Hollingsworth, S., Marquardt, T., Barnes, A., Smith, R., Mcshane, R., Turner, E. H., & Cipriani, A. (2021). Ketamine and other glutamate receptor modulators for depression in adults with unipolar major depressive disorder. *Cochrane Database of Systematic Reviews*, *9*(9), CD011612. https://doi.org/10.1002/14651858.CD011612.pub3

Dillon, D. G., & Pizzagalli, D. A. (2018). Mechanisms of memory disruption in depression. *Trends in Neurosciences*, *41*(3), 137–149. https://doi.org/10.1016/j.tins.2017.12.006

Duman, R. S., & Aghajanian, G. K. (2012). Synaptic dysfunction in depression: Potential therapeutic targets. *Science*, *338*(6103), 68–72. https://doi.org/10.1126/science.1222939

Dumlu, S. N., Ademoglu, A., & Sun, W. (2020). Investigation of functional variability and connectivity in temporal lobe epilepsy: A resting state fMRI study. *Neuroscience Letters*, *733*, 135076. https://doi.org/10.1016/j.neulet.2020.135076

Fee, C., Banasr, M., & Sibille, E. (2017). Somatostatin-positive gamma-aminobutyric acid interneuron deficits in depression: Cortical microcircuit and therapeutic perspectives. *Biological Psychiatry*, *82*(8), 549–559. https://doi.org/10.1016/j.biopsych.2017.05.024

Fields, R. D. (2008). White matter in learning, cognition and psychiatric disorders. *Trends in Neurosciences*, *31*(7), 361–370. https://doi.org/10.1016/j.tins.2008.04.001

Finn, E. S., & Todd Constable, R. (2016). Individual variation in functional brain connectivity: Implications for personalized approaches to psychiatric disease. *Dialogues in Clinical Neuroscience*, *18*(3), 277–287. https://doi.org/10.31887/DCNS.2016.18.3/efinn

Flint, J., & Kendler, K. S. (2014). The genetics of major depression. *Neuron*, *81*(3), 484–503. https://doi.org/10.1016/j.neuron.2014.01.027

Gao, W., Elton, A., Zhu, H., Alcauter, S., Smith, J. K., Gilmore, J. H., & Lin, W. (2014). Intersubject variability of and genetic effects on the brain's functional connectivity during infancy. *The Journal of Neuroscience*, *34*(34), 11288–11296. https://doi.org/10.1523/JNEUROSCI.5072-13.2014

Golan, M., Schreiber, G., & Avissar, S. (2013). Antidepressant-induced differential ubiquitination of beta-arrestins 1 and 2 in mononuclear leucocytes of patients with depression. *The International Journal of Neuropsychopharmacology*, *16*(8), 1745–1754. https://doi.org/10.1017/S1461145713000291

Gottlieb, D. J., O'Connor, G. T., & Wilk, J. B. (2007). Genome-wide association of sleep and circadian phenotypes. *BMC Medical Genetics*, *8*(Suppl 1), S9. https://doi.org/10.1186/1471-2350-8-S1-S9

Hashimoto, K. (2019). Rapid-acting antidepressant ketamine, its metabolites and other candidates: A historical overview and future perspective. *Psychiatry and Clinical Neurosciences*, *73*(10), 613–627. https://doi.org/10.1111/pcn.12902

Hawrylycz, M. J., Lein, E. S., Guillozet-Bongaarts, A. L., Shen, E. H., Ng, L., Miller, J. A., van de Lagemaat, L. N., Smith, K. A., Ebbert, A., Riley, Z. L., Abajian, C., Beckmann, C. F., Bernard, A., Bertagnolli, D., Boe, A. F., Cartagena, P. M., Chakravarty, M. M., Chapin, M., Chong, J., … Jones, A. R. (2012). An anatomically comprehensive atlas of the adult human brain transcriptome. *Nature*, *489*(7416), 391–399. https://doi.org/10.1038/nature11405

Horien, C., Shen, X., Scheinost, D., & Constable, R. T. (2019). The individual functional connectome is unique and stable over months to years. *NeuroImage*, *189*, 676–687. https://doi.org/10.1016/j.neuroimage.2019.02.002

Hou, Z., Jiang, W., Li, F., Liu, X., Hou, Z., Yin, Y., Zhang, H., Zhang, H., Xie, C., Zhang, Z., Kong, Y., & Yuan, Y. (2023). Linking individual variability in functional brain connectivity to polygenic risk in major depressive disorder. *Journal of Affective Disorders*, *329*, 55–63. https://doi.org/10.1016/j.jad.2023.02.104

Howard, D. M., Adams, M. J., Clarke, T. K., Hafferty, J. D., Gibson, J., Shirali, M., Coleman, J. R. I., Hagenaars, S. P., Ward, J., Wigmore, E. M., Alloza, C., Shen, X., Barbu, M. C., Xu, E. Y., Whalley, H. C., Marioni, R. E., Porteous, D. J., Davies, G., Deary, I. J., … McIntosh, A. M. (2019). Genome-wide meta-analysis of depression identifies 102 independent variants and highlights the importance of the prefrontal brain regions. *Nature Neuroscience*, *22*(3), 343–352. https://doi.org/10.1038/s41593-018-0326-7

Iadecola, C. (2017). The neurovascular unit coming of age: A journey through neurovascular coupling in health and disease. *Neuron*, *96*(1), 17–42. https://doi.org/10.1016/j.neuron.2017.07.030

Ji, G. J., Liao, W., Chen, F. F., Zhang, L., & Wang, K. (2017). Low-frequency blood oxygen level-dependent fluctuations in the brain white matter: More than just noise. *Sci Bull (Beijing)*, *62*(9), 656–657. https://doi.org/10.1016/j.scib.2017.03.021

Jorgensen, A., Krogh, J., Miskowiak, K., Bolwig, T. G., Kessing, L. V., Fink-Jensen, A., Nordentoft, M., Henriksen, T., Weimann, A., Poulsen, H. E., & Jorgensen, M. B. (2013). Systemic oxidatively generated DNA/RNA damage in clinical depression: Associations to symptom severity and response to electroconvulsive therapy. *Journal of Affective Disorders*, *149*(1–3), 355–362. https://doi.org/10.1016/j.jad.2013.02.011

Karras, J. R., Paisie, C. A., & Huebner, K. (2014). Replicative stress and the FHIT gene: Roles in tumor suppression, genome stability and prevention of carcinogenesis. *Cancers (Basel)*, *6*(2), 1208–1219. https://doi.org/10.3390/cancers6021208

Kessler, R. C., Berglund, P., Borges, G., Nock, M., & Wang, P. S. (2005). Trends in suicide ideation, plans, gestures, and attempts in the United States, 1990-1992 to 2001-2003. *Jama*, *293*(20), 2487–2495. https://doi.org/10.1001/jama.293.20.2487

Korgaonkar, M. S., Williams, L. M., Song, Y. J., Usherwood, T., & Grieve, S. M. (2014). Diffusion tensor imaging predictors of treatment outcomes in major depressive disorder. *The British Journal of Psychiatry*, *205*(4), 321–328. https://doi.org/10.1192/bjp.bp.113.140376

Koshiyama, D., Fukunaga, M., Okada, N., Morita, K., Nemoto, K., Usui, K., Yamamori, H., Yasuda, Y., Fujimoto, M., Kudo, N., Azechi, H., Watanabe, Y., Hashimoto, N., Narita, H., Kusumi, I., Ohi, K., Shimada, T., Kataoka, Y., Yamamoto, M., … COCORO. (2020). White matter microstructural alterations across four major psychiatric disorders: Mega-analysis study in 2937 individuals. *Molecular Psychiatry*, *25*(4), 883–895. https://doi.org/10.1038/s41380-019-0553-7

Koshiyama, D., Fukunaga, M., Okada, N., Morita, K., Nemoto, K., Yamashita, F., Yamamori, H., Yasuda, Y., Matsumoto, J., Fujimoto, M., Kudo, N., Azechi, H., Watanabe, Y., Kasai, K., & Hashimoto, R. (2020). Association between the superior longitudinal fasciculus and perceptual organization and working memory: A diffusion tensor imaging study. *Neuroscience Letters*, *738*, 135349. https://doi.org/10.1016/j.neulet.2020.135349

Krishnan, A., Williams, L. J., McIntosh, A. R., & Abdi, H. (2011). Partial least squares (PLS) methods for neuroimaging: A tutorial and review. *NeuroImage*, *56*(2), 455–475. https://doi.org/10.1016/j.neuroimage.2010.07.034

Kumar, P., Kumar, D., Jha, S. K., Jha, N. K., & Ambasta, R. K. (2016). Ion channels in neurological disorders. *Advances in Protein Chemistry and Structural Biology*, *103*, 97–136. https://doi.org/10.1016/bs.apcsb.2015.10.006

Lemon, R. N. (2008). Descending pathways in motor control. *Annual Review of Neuroscience*, *31*, 195–218. https://doi.org/10.1146/annurev.neuro.31.060407.125547

Lepine, J. P., & Briley, M. (2011). The increasing burden of depression. *Neuropsychiatric Disease and Treatment*, *7*(Suppl 1), 3–7. https://doi.org/10.2147/NDT.S19617

Li, J., Biswal, B. B., Meng, Y., Yang, S., Duan, X., Cui, Q., Chen, H., & Liao, W. (2020). A neuromarker of individual general fluid intelligence from the white-matter functional connectome. *Translational Psychiatry*, *10*(1), 147. https://doi.org/10.1038/s41398-020-0829-3

Li, J., Chen, H., Fan, F., Qiu, J., Du, L., Xiao, J., Duan, X., Chen, H., & Liao, W. (2020). White-matter functional topology: A neuromarker for classification and prediction in unmedicated depression. *Translational Psychiatry*, *10*(1), 365. https://doi.org/10.1038/s41398-020-01053-4

Li, J., Seidlitz, J., Suckling, J., Fan, F., Ji, G. J., Meng, Y., Yang, S., Wang, K., Qiu, J., Chen, H., & Liao, W. (2021). Cortical structural differences in major depressive disorder correlate with cell type-specific transcriptional signatures. *Nature Communications*, *12*(1), 1647. https://doi.org/10.1038/s41467-021-21943-5

Li, J., Wu, G. R., Li, B., Fan, F., Zhao, X., Meng, Y., Zhong, P., Yang, S., Biswal, B. B., Chen, H., & Liao, W. (2021). Transcriptomic and macroscopic architectures of intersubject functional variability in human brain white-matter. *Communications Biology*, *4*(1), 1417. https://doi.org/10.1038/s42003-021-02952-y

Li, L., Wei, Y., Zhang, J., Ma, J., Yi, Y., Gu, Y., Li, L. M. W., Lin, Y., & Dai, Z. (2021). Gene expression associated with individual variability in intrinsic functional connectivity. *NeuroImage*, *245*, 118743. https://doi.org/10.1016/j.neuroimage.2021.118743

Ma, Y. J., Wang, D. F., Yuan, M., Zhang, X. J., Long, J., Chen, S. B., Wu, Q. X., Wang, X. Y., Patel, M., Verrico, C. D., Liu, T. Q., & Zhang, X. Y. (2019). The prevalence, metabolic disturbances and clinical correlates of recent suicide attempts in Chinese inpatients with major depressive disorder. *BMC Psychiatry*, *19*(1), 144. https://doi.org/10.1186/s12888-019-2131-6

Malhi, G. S., & Mann, J. J. (2018). Depression. *Lancet*, *392*(10161), 2299–2312. https://doi.org/10.1016/S0140-6736(18)31948-2

Manelis, A., Soehner, A., Halchenko, Y. O., Satz, S., Ragozzino, R., Lucero, M., Swartz, H. A., Phillips, M. L., & Versace, A. (2021). White matter abnormalities in adults with bipolar disorder type-II and unipolar depression. *Scientific Reports*, *11*(1), 7541. https://doi.org/10.1038/s41598-021-87069-2

Matsuoka, K., Yasuno, F., Kishimoto, T., Yamamoto, A., Kiuchi, K., Kosaka, J., Nagatsuka, K., Iida, H., & Kudo, T. (2017). Microstructural differences in the corpus callosum in patients with bipolar disorder and major depressive disorder. *The Journal of Clinical Psychiatry*, *78*(1), 99–104. https://doi.org/10.4088/JCP.15m09851

Millan, M. J., Agid, Y., Brune, M., Bullmore, E. T., Carter, C. S., Clayton, N. S., Connor, R., Davis, S., Deakin, B., DeRubeis, R. J., Dubois, B., Geyer, M. A., Goodwin, G. M., Gorwood, P., Jay, T. M., Joëls, M., Mansuy, I. M., Meyer-Lindenberg, A., Murphy, D., … Young, L. J. (2012). Cognitive dysfunction in psychiatric disorders: Characteristics, causes and the quest for improved therapy. *Nature Reviews. Drug Discovery*, *11*(2), 141–168. https://doi.org/10.1038/nrd3628

Morgan, S. E., Seidlitz, J., Whitaker, K. J., Romero-Garcia, R., Clifton, N. E., Scarpazza, C., van Amelsvoort, T., Marcelis, M., van Os, J., Donohoe, G., Mothersill, D., Corvin, A., Pocklington, A., Raznahan, A., McGuire, P., Vértes, P. E., & Bullmore, E. T. (2019). Cortical patterning of abnormal morphometric similarity in psychosis is associated with brain expression of schizophrenia-related genes. *Proceedings of the National Academy of Sciences of the United States of America*, *116*(19), 9604–9609. https://doi.org/10.1073/pnas.1820754116

Mueller, S., Wang, D., Fox, M. D., Yeo, B. T., Sepulcre, J., Sabuncu, M. R., Shafee, R., Lu, J., & Liu, H. (2013). Individual variability in functional connectivity architecture of the human brain. *Neuron*, *77*(3), 586–595. https://doi.org/10.1016/j.neuron.2012.12.028

Nagy, C., Maitra, M., Tanti, A., Suderman, M., Theroux, J. F., Davoli, M. A., Perlman, K., Yerko, V., Wang, Y. C., Tripathy, S. J., Pavlidis, P., Mechawar, N., Ragoussis, J., & Turecki, G. (2020). Single-nucleus transcriptomics of the prefrontal cortex in major depressive disorder implicates oligodendrocyte precursor cells and excitatory neurons. *Nature Neuroscience*, *23*(6), 771–781. https://doi.org/10.1038/s41593-020-0621-y

Nardou, R., Lewis, E. M., Rothhaas, R., Xu, R., Yang, A., Boyden, E., & Dolen, G. (2019). Oxytocin-dependent reopening of a social reward learning critical period with MDMA. *Nature*, *569*(7754), 116–120. https://doi.org/10.1038/s41586-019-1075-9

Niogi, S., Mukherjee, P., Ghajar, J., & McCandliss, B. D. (2010). Individual differences in distinct components of attention are linked to anatomical variations in distinct white matter tracts. *Frontiers in Neuroanatomy*, *4*, 2. https://doi.org/10.3389/neuro.05.002.2010

Northoff, G., & Sibille, E. (2014). Why are cortical GABA neurons relevant to internal focus in depression? A cross-level model linking cellular,

biochemical and neural network findings. *Molecular Psychiatry*, *19*(9), 966–977. https://doi.org/10.1038/mp.2014.68

Pedersen, W. S., Dean, D. C., Adluru, N., Gresham, L. K., Lee, S. D., Kelly, M. P., Mumford, J. A., Davidson, R. J., & Schaefer, S. M. (2022). Individual variation in white matter microstructure is related to better recovery from negative stimuli. *Emotion*, *22*(2), 244–257. https://doi.org/10.1037/emo0000996

Roland, J. L., Snyder, A. Z., Hacker, C. D., Mitra, A., Shimony, J. S., Limbrick, D. D., Raichle, M. E., Smyth, M. D., & Leuthardt, E. C. (2017). On the role of the corpus callosum in interhemispheric functional connectivity in humans. *Proceedings of the National Academy of Sciences of the United States of America*, *114*(50), 13278–13283. https://doi.org/10.1073/pnas.1707050114

Schmahmann, J. D., Pandya, D. N., Wang, R., Dai, G., D'Arceuil, H. E., de Crespigny, A. J., & Wedeen, V. J. (2007). Association fibre pathways of the brain: Parallel observations from diffusion spectrum imaging and autoradiography. *Brain*, *130*(Pt 3), 630–653. https://doi.org/10.1093/brain/awl359

Segarra, M., Aburto, M. R., Hefendehl, J., & Acker-Palmer, A. (2019). Neurovascular interactions in the nervous system. *Annual Review of Cell and Developmental Biology*, *35*, 615–635. https://doi.org/10.1146/annurev-cellbio-100818-125142

Seidlitz, J., Nadig, A., Liu, S., Bethlehem, R. A. I., Vertes, P. E., Morgan, S. E., Váša, F., Romero-Garcia, R., Lalonde, F. M., Clasen, L. S., Blumenthal, J. D., Paquola, C., Bernhardt, B., Wagstyl, K., Polioudakis, D., de la Torre-Ubieta, L., Geschwind, D. H., Han, J. C., Lee, N. R., … Raznahan, A. (2020). Transcriptomic and cellular decoding of regional brain vulnerability to neurogenetic disorders. *Nature Communications*, *11*(1), 3358. https://doi.org/10.1038/s41467-020-17051-5

Shaffer, C., Westlin, C., Quigley, K. S., Whitfield-Gabrieli, S., & Barrett, L. F. (2022). Allostasis, action, and affect in depression: Insights from the theory of constructed emotion. *Annual Review of Clinical Psychology*, *18*, 553–580. https://doi.org/10.1146/annurev-clinpsy-081219-115627

Smith, S. M., Nichols, T. E., Vidaurre, D., Winkler, A. M., Behrens, T. E., Glasser, M. F., Ugurbil, K., Barch, D. M., Van Essen, D. C., & Miller, K. L. (2015). A positive-negative mode of population covariation links brain connectivity, demographics and behavior. *Nature Neuroscience*, *18*(11), 1565–1567. https://doi.org/10.1038/nn.4125

Sullivan, E. V., Zahr, N. M., Rohlfing, T., & Pfefferbaum, A. (2010). Fiber tracking functionally distinct components of the internal capsule. *Neuropsychologia*, *48*(14), 4155–4163. https://doi.org/10.1016/j.neuropsychologia.2010.10.023

Sullivan, P. F., Neale, M. C., & Kendler, K. S. (2000). Genetic epidemiology of major depression: Review and meta-analysis. *The American Journal of Psychiatry*, *157*(10), 1552–1562. https://doi.org/10.1176/appi.ajp.157.10.1552

Sun, X., Liu, J., Ma, Q., Duan, J., Wang, X., Xu, Y., Xu, Z., Xu, K., Wang, F., Tang, Y., He, Y., & Xia, M. (2021). Disrupted intersubject variability architecture in functional connectomes in schizophrenia. *Schizophrenia Bulletin*, *47*(3), 837–848. https://doi.org/10.1093/schbul/sbaa155

Thomas, C., Avidan, G., Humphreys, K., Jung, K. J., Gao, F., & Behrmann, M. (2009). Reduced structural connectivity in ventral visual cortex in congenital prosopagnosia. *Nature Neuroscience*, *12*(1), 29–31. https://doi.org/10.1038/nn.2224

Vasa, F., Seidlitz, J., Romero-Garcia, R., Whitaker, K. J., Rosenthal, G., Vertes, P. E., Shinn, M., Alexander-Bloch, A., Fonagy, P., Dolan, R. J., Jones, P. B., Goodyer, I. M., NSPN Consortium, Sporns, O., & Bullmore, E. T. (2018). Adolescent tuning of association cortex in human structural brain networks. *Cerebral Cortex*, *28*(1), 281–294. https://doi.org/10.1093/cercor/bhx249

Williams, J. B. (1988). A structured interview guide for the Hamilton depression rating scale. *Archives of General Psychiatry*, *45*(8), 742–747. https://doi.org/10.1001/archpsyc.1988.01800320058007

Won, E., Choi, S., Kang, J., Kim, A., Han, K. M., Chang, H. S., Tae, W. S., Son, K. R., Joe, S. H., Lee, M. S., & Ham, B. J. (2016). Association between reduced white matter integrity in the corpus callosum and serotonin transporter gene DNA methylation in medication-naive patients with major depressive disorder. *Translational Psychiatry*, *6*(8), e866. https://doi.org/10.1038/tp.2016.137

Xu, E. P., Nguyen, L., Leibenluft, E., Stange, J. P., & Linke, J. O. (2023). A meta-analysis on the uncinate fasciculus in depression. *Psychological Medicine*, *53*(7), 2721–2731. https://doi.org/10.1017/S0033291723000107

Xue, K., Liang, S., Yang, B., Zhu, D., Xie, Y., Qin, W., Liu, F., Zhang, Y., & Yu, C. (2022). Local dynamic spontaneous brain activity changes in first-episode, treatment-naive patients with major depressive disorder and their associated gene expression profiles. *Psychological Medicine*, *52*(11), 2052–2061. https://doi.org/10.1017/S0033291720003876

Yarkoni, T., Poldrack, R. A., Nichols, T. E., Van Essen, D. C., & Wager, T. D. (2011). Large-scale automated synthesis of human functional neuroimaging data. *Nature Methods*, *8*(8), 665–670. https://doi.org/10.1038/nmeth.1635

Zhuo, C., Li, G., Lin, X., Jiang, D., Xu, Y., Tian, H., Wang, W., & Song, X. (2019). The rise and fall of MRI studies in major depressive disorder. *Translational Psychiatry*, *9*(1), 335. https://doi.org/10.1038/s41398-019-0680-6

SUPPORTING INFORMATION

Additional supporting information can be found online in the Supporting Information section at the end of this article.

How to cite this article: Gai, Q., Chu, T., Li, Q., Guo, Y., Ma, H., Shi, Y., Che, K., Zhao, F., Dong, F., Li, Y., Xie, H., & Mao, N. (2024). Altered intersubject functional variability of brain white-matter in major depressive disorder and its association with gene expression profiles. *Human Brain Mapping*, *45*(5), e26670. https://doi.org/10.1002/hbm.26670